FEBS Letters 583 (2009) 3419–3424

FEBS Letters

journal homepage: www.FEBSLetters.org

Cx40.8, a Cx43-like protein, forms gap junction channels inefficiently and may require Cx43 for its association at the plasma membrane

Sarah V. Gerhart, Rebecca Jefferis, M. Kathryn Iovine *

Lehigh University, Department of Biological Sciences, 111 Research Drive, Iacocca B-217, Bethlehem, PA 18015, United States

ARTICLE INFO

Article history:
Received 12 August 2009
Revised 22 September 2009
Accepted 26 September 2009
Available online 4 October 2009

Edited by Lukas Huber

Keywords:
Connexin
Cx40.8
Cx43
Gap junction
Zebrafish
Short fin

ABSTRACT

In addition to having a Cx43 ortholog, the zebrafish genome also contains a Cx43-like gene, Cx40.8. Here, we investigate the expression of *cx40.8* in zebrafish fins and the function of Cx40.8 in HeLa cells. We find that *cx40.8* is present in the same population of dividing cells as *cx43*. Unlike Cx43, dye coupling assays suggest that Cx40.8 only inefficiently forms functional gap junction channels. However, co-transfection reveals that Cx40.8 can co-localize with Cx43 in gap junction plaques, and that the resulting plaques contain functional gap junction channels. Together, these data suggest the possibility that Cx40.8 may functionally interact with Cx43 to regulate cell proliferation in vivo.

Structured summary:
MINT-7266123: *cx40.8* (genbank_protein_gi:68354404) and *cx43* (uniprotkb:O57474) *colocalize* (MI:0403) by *fluorescence microscopy* (MI:0416)

1. Introduction

Connexins, the subunits of gap junction channels, are part of a large multigene family consisting of about 20 genes in mammals [1]. Connexins are integral membrane proteins that consist of four transmembrane domains, two extracellular loops, one cytoplasmic loop, and cytoplasmic amino- and carboxy-termini. Six connexin proteins oligomerize to form one connexon (or hemichannel), and the docking of two connexons at the plasma membranes of neighboring cells forms a single gap junction channel. Gap junction channels typically aggregate into plaques containing about 100–1000 channels, allowing the passage of ions and small molecules (<1200 Da) between adjacent cells. Interestingly, most tissues express a unique assortment of 2–7 connexin genes, suggesting that distinct homomeric and heteromeric gap junction channels contribute to cell–cell coupling [2]. Further, channel composition can determine metabolite selectivity and specificity [3–5]. Therefore, one possibility is that regulated hetero-oligomerization of different connexin isotypes may in turn regulate tissue function.

Gap junction intercellular communication (GJIC) is necessary for normal tissue development, evidenced by the identification of mutations in connexins causing such disease phenotypes as deafness, skin disorders, peripheral neuropathies, and cataracts [2,6,7]. In particular, missense mutations in human *CX43* cause the craniofacial and limb skeletal malformations associated with oculodentodigital dysplasia (ODDD) [8]. ODDD is transmitted as an autosomal dominant disease, suggesting that mutant forms of Cx43 may hetero-oligomerize with wild-type Cx43, perhaps poisoning Cx43 gap junction channels [2,9]. Mutations in zebrafish *cx43* also cause skeletal phenotypes, including short bony fin ray segments associated with the *short fin* phenotype [10,11]. In addition to the sof^{b123} allele that has reduced mRNA and protein levels [12,13], three non-complementing ENU-induced alleles were shown to cause missense mutations (sof^{j7e1} codes Cx43-F30V, sof^{j7e2} codes Cx43-P191S, and sof^{j7e3} codes Cx43-F209I). Each missense allele can form gap junction plaques, but channels exhibit aberrant ionic coupling properties [11]. Indeed, recent studies on the zebrafish *cx43* mutations reveal a correlation between segment length, level of proliferation, and GJIC [11,13]. Therefore, the zebrafish fin represents an excellent model system to understand how changes in GJIC may lead to important developmental phenotypes, including bone growth.

The zebrafish caudal fin consists of 16–18 bony rays, and fin length depends on the number and size of numerous segments [14]. Fins also have the capacity for rapid growth during

Abbreviations: ODDD, oculodentodigital dysplasia; GJIC, gap junction intercellular communication; ISH, in situ hybridization; H3P, histone-3-phosphate; dpa, days post amputation

* Corresponding author. Fax: +1 610 758 4004.
E-mail address: mki3@lehigh.edu (M.K. Iovine).

0014-5793/$36.00 © 2009 Federation of European Biochemical Societies. Published by Elsevier B.V. All rights reserved.
doi:10.1016/j.febslet.2009.09.054

regeneration. Amputation is immediately followed by wound healing, and the regeneration blastema is next established [15,16]. The blastema is a specialized structure composed primarily of proliferating cells, and is required for outgrowth. Dividing cells differentiate to contribute to all the tissues of the fin. Expression of *cx43* is identified both in the proliferating cells of the blastema and in differentiated cells surrounding fin ray joints [10]. Further, all of the *sof* alleles exhibit reduced levels of cell proliferation. This and other data suggests that Cx43-based GJIC may be required to establish the population of dividing cells [13]. Therefore, it is important to understand how Cx43-mediated coupling is regulated in this tissue.

The zebrafish genome includes a large connexin gene family ($n = 37$) [17], almost twice the size of human ($n = 21$) and mouse ($n = 20$) families. Phylogenetic analysis revealed that 23 of the zebrafish connexins were a result of the additional whole genome duplication in the teleost lineage [18], while the remaining 14 may have arisen by individual gene duplication events and subsequent divergence [17]. Here we describe the zebrafish *cx43*-like gene, *cx40.8*. The *cx40.8* gene shares 79% amino acid (Fig. 1) and 80% nucleotide identity with *cx43*. Given the close phylogenetic relationship, Cx40.8 may be compatible to form heteromeric channels with Cx43 and directly modify Cx43-based GJIC. Indeed, heteromeric gap junctions often exhibit distinct channel properties from either homomeric form [3,19–21]. Here, we provide an initial characterization of Cx40.8 expression and function. Results from these and continued studies may provide an endogenous model system to understand how closely related connexins regulate GJIC, and/or how missense alleles may modify wild-type activity.

2. Materials and methods

2.1. Fish maintenance

The fish used in this study were derived from the C32 strain and were raised in a 14 light:10 dark photoperiod at 25 °C [22].

2.2. In situ hybridization (ISH)

The coding sequence for *cx40.8* was amplified (F—GAATCTCGAGATGGGTGACTGGAGCGCACTGG; R—GAATGTCGACTGGATGTCAAGATCATCCGGCC), TA-cloned into pGEMT, and sequenced. Digoxigenin-labeled antisense probe for *cx40.8* was generated. Tissue was fixed overnight with 4% paraformaldehyde in PBS and stored in 100% methanol at −20 °C. Gradual aqueous washes were completed in methanol/PBST. Tissue was treated with 5 μg/ml proteinase K (5 min for embryos; 45 min for fins) and re-fixed for 20 min. Prehybridization (50% formamide, 5× SSC, 10 mM citric

```
Dr.Cx43         MGDWSALGRLLDKVQAYSTAGGKVWLSVLFIFRILVLGTAVESAWGDEQSAFKCNTQQPG 60
Hs.Cx43         MGDWSALGKLLDKVQAYSTAGGKVWLSVLFIFRILLLGTAVESAWGDEQSAFRCNTQQPG 60
Dr.Cx40.8       MGDWSALGKLLDKVQAYSTAGGKVWLSVLFIFRILVLGTAVESAWGDEQSAFKCNTLQPG 60
                ********:**************************:****************:*** ***

Dr.Cx43         CENVCYDKSFPISHVRFWVLQIIFVSTPTLLYLAHVFYLMRKEEKLNRKEEELKAVQNDG 120
Hs.Cx43         CENVCYDKSFPISHVRFWVLQIIFVSVPTLLYLAHVFYVMRKEEKLNKKEEELKVAQTDG 120
Dr.Cx40.8       CENVCYDKSFPISHVRFWVLQIIFVSMPTLLYLSHVVFLMNKEEKLNKKEDKLRDIQSKG 120
                ************************* ******:**.::*.******:**::*:  *..*

Dr.Cx43         GDVELHLKKIELKKFKHGLEEHGKVKMKGSLLRTYIFSIIFKSICEVVFLVIQWYLYGFS 180
Hs.Cx43         VNVDMHLKQIEIKKFKYGIEEHGKVKMRGGLLRTYIISILFKSIFEVAFLLIQWYIYGFS 180
Dr.Cx40.8       GDVDVLLRKIETRKFKYGLEDHGKIKMRGGIFYTYIVSIVLKSVFEIVFLLIQWHLYGFK 180
                 :*:: *::** :***:*:*:***:**:*.:: ***.**::**: *:.**:***::***.
                                                              ↓
Dr.Cx43         LSAVYTCERTPCPHRVDCFLSRPTEKTIFIIFMLVVSLFSLLLNIIELFYVLFKRIKDRV 240
Hs.Cx43         LSAVYTCKRDPCPHQVDCFLSRPTEKTIFIIFMLVVSLVSLALNIIELFYVFFKGVKDRV 240
Dr.Cx40.8       LSAVYTCEKFPCPHKVDCFLSRPTEKTVFIIFMLVVSLVSLALNVFEFFYVIFKRMKDQI 240
                *******:: ****:************:**********.** **::*:***:** :**::

Dr.Cx43         KSRQNTQFPT-GTLSPTPKELSTTKYAYYNGCSSPTAPLSPMSPPGYKLATGERTN-SCR 298
Hs.Cx43         KGKSDPYHATSGALSP-AKDCGSQKYAYFNGCSSPTAPLSPMSPPGYKLVTGDRNNSSCR 299
Dr.Cx40.8       R-ESEKKFDSACNIKPCPRNLSG--YEYYNDCSAPVPNL------GYNLDTVDKSN-SSD 290
                : ..:  . :   :.* .:: .   * *:*.**:*.. *      **:* * ::.* *.

Dr.Cx43         NYNKQANEQNWANYSTEQNRLGQNGSTISNSHAQAFDYPDDTHEHKKLTPGHELQPLALI 358
Hs.Cx43         NYNKQASEQNWANYSAEQNRMGQAGSTISNSHAQPFDFPDDNQNSKKLAAGHELQPLAIV 359
Dr.Cx40.8       NYDKQANEQNWTNYSTEQNQLG---------HSQRFPYP------EKVTLGKDLLLLKEL 335
                **:***.****:***:***::*          *:* * :*      :*:: *::*  *  :

Dr.Cx43         DARPCSRASSRMSSRARPDDLDV 381
Hs.Cx43         DQRPSSRASSRASSRPRPDDLEI 382
Dr.Cx40.8       EPRP----SSRASSRARPDDLDI 354
                : **    *** ***.*****::
```

Fig. 1. Alignment of Cx43-related connexins. Amino acid alignments of human (Hs) Cx43, zebrafish (Dr) Cx43, and zebrafish (Dr) Cx40.8 were completed using ClustalW. The stars indicate amino acid identity, 2 dots indicates strong conservation, 1 dot indicates moderate conservation, and dashes indicate gaps. The arrow identifies the start of the carboxy-tail.

acid, 0.1% Tween20) occurred for 1 h at 65 °C, and hybridization in the presence of digoxigenin-labeled antisense probes was completed overnight. Gradual washes into 0.2× SSC were followed by gradual washes into PBST. Anti-digoxigenin Fab fragments (pre-absorbed against zebrafish tissue) were used at 1:5000 overnight. Extensive washes in PBST followed by three short washes in staining buffer (100 mM Tris, pH 9.5, 50 mM $MgCl_2$, 100 mM NaCl, 0.1% Tween20, pH 9.0) were completed. Tissue was next transferred to staining solution (staining buffer plus 0.22 mg/ml NBT and 0.175 mg/ml BCIP) and development proceeded until purple color was observed.

2.3. qRT-PCR analysis

Trizol reagent (Gibco) was used to isolate mRNA from 5 days - post amputation (dpa) regenerating fins (5–10 fins were pooled) and first strand cDNA was prepared using oligodT (12–15) and reverse transcriptase. Dilutions of template cDNA were prepared (1:5, 1:50, 1:500, 1:5000). Oligos were designed for *cx40.8* using Primer Express software (F—ATTACAATGACTGCTCGGCCC; R—TGCTCATTAGCCTGCTTGTCG). Oligos for *cx43* and internal standard *ker4* were described previously [12]. All amplicons were amplified independently using the Power SYBR green PCR master mix (Applied Biosystems). Samples were run in triplicate on the ABI7300 Real Time PCR system and the average cycle number (C_T) was determined for each amplicon. Delta CT (ΔC_T) values represent normalized *cx43* or *cx40.8* levels with respect to *keratin4*. Delta Delta CT ($\Delta\Delta CT$) values represent expression levels of the test sample (*sof*^{b123}) minus the expression levels of the calibrator sample (wild-type) for either *cx43* or *cx40.8*. The fold-change was calculated using the double ΔC_T method (i.e. using the equation $2^{-\Delta\Delta CT}$). Three independent experiments were completed.

2.4. Detection of mitotic cells using histone-3-phosphate (H3P)

This method identifies mitotic cells by detecting a phosphorylated form of serine-10 (H3P) that is present only during mitosis [23]. Following processing for *cx40.8* ISH, the fins were washed in PBS then treated with 1 mg/ml collagenase in PBS for 45 min at room temperature and blocked using a 0.5% BSA in PBS solution with 0.1% Triton-X. A rabbit antibody against anti-phosphohistone H3 (H3P, Upstate Biotechnology) was diluted 1:100 in block and fins were incubated overnight at 4 °C. Following a series of washes in block, fins were incubated with an anti-rabbit antibody conjugated to Alexa-546 (Molecular Probes, diluted 1:200 in block) for 2.5 h at room temperature. Washes were performed in block followed by cryosectioning to detect cells doubly-labeled for *cx40.8* and H3P. All H3P-positive cells within the distal-most 250 μm were identified as *cx40.8* positive or negative [13].

2.5. Plasmid construction and HeLa cell transfection

The *cx40.8* coding sequence was excised from pGEMT using XhoI and SalI restriction endonucleases engineered into the primers used for the initial amplification (see above under Section 2.2), and subcloned into p-mApple or pEGFP-N1 (Clontech). For *cx43* constructs, the coding sequence from Cx43-N1-EGFP (described in [11]) was subcloned into the EcoRI site of p-mApple. Plasmid DNA was prepared using the MiniPrep Plasmid Purification kit (Qiagen).

HeLa cells were stored at 5% CO_2 and 37 °C and grown in tissue culture dishes with minimal essential media supplemented with 10% FBS, antibiotics, and antimycotics (Invitrogen). The cells were seeded onto poly-L-lysine coverglasses, incubated overnight, then transfected for 3 h using either 2 μg of Cx40.8-EGFP-N1 or Cx40.8-mApple using Superfect (Qiagen). For double transfections, a combination of 1 μg Cx40.8-EGFP-N1 and 1 μg Cx43-mApple was co-transfected using the same procedure. Transfected cell pairs were evaluated by confocal microscopy (Zeiss).

2.6. Dye coupling assays

Following transfection (t = 21 h), transfected cell pairs were identified and a single cell within the pair was injected with propidium iodide (PI, MW = 668.4) using the Eppendorf FemtoJet microinjector and Eppendorf InjectMan N12 micromanipulator. Dye transfer to the non-injected cell of the pair was indicative of functional gap junction channels, and the percentage of cell pairs that showed dye transfer was calculated for each cell culture dish. A total of 25 cell pairs were evaluated for Cx40.8-EGFP and for doubly-transfected cells. The average and standard deviation from three trials for each experiment was determined. Statistical significance was calculated using the Student's t-test.

3. Results and discussion

3.1. Cx40.8 is expressed in the same population of cells as Cx43

First, we examined *cx40.8* expression in regenerating wild-type fins by ISH. Following whole mount staining and cryosectioning, we found that *cx40.8* is expressed in the distal mesenchymal compartment (Fig. 2A and C), consistent with the location of proliferating cells and similar to the location of *cx43* expression [10]. Given the high percentage of nucleotide similarity between *cx40.8* and *cx43*, it was necessary to rule out the possibility that the above observations were due to cross-hybridization of the *cx40.8* probe with the *cx43* mRNA. Previously, we found that *cx43* is undetectable in *short fin* (*sof*^{b123}) regenerating fins by ISH [10]. If the *cx40.8* probe hybridizes to *cx43* (i.e. in addition to or instead of hybridizing to the *cx40.8* mRNA), we would expect that *cx40.8* might also fail to be detected in *sof*^{b123}fins. Instead the *cx40.8* expression pattern in *sof*^{b123} (Fig. 2B) is similar to the wild-type pattern, indicating that the *cx40.8* probe identifies the correct target sequence and does not rely on the presence of *cx43* mRNA for detection.

The expression domain of *cx43* and *cx40.8* is consistent with the population of proliferating cells in the regeneration blastema. Previous studies revealed that 89% of the H3P-positive mitotic cells in this region also express *cx43* [13]. To determine if *cx40.8* is also expressed in actively dividing cells, regenerating fins were processed for *cx40.8* ISH and H3P detection. Cryosectioning of doubly-stained fins revealed that 80.6% of mesenchymal H3P-positive cells also expressed *cx40.8* (n = 31 H3P cells, Fig. 2D). The finding that *cx40.8* and *cx43* are expressed in the same compartment, together with the finding that *cx40.8* is expressed in mitotic cells, suggests that *cx40.8* is expressed in the same population of proliferating cells as *cx43*.

3.2. Expression levels of cx40.8 are unchanged in sof^{b123}

Since *cx40.8* and *cx43* appear to be expressed in the same cells, the expression levels of these genes may be co-regulated. To test this possibility, qRT-PCR was used to compare the relative levels of *cx43* and *cx40.8* mRNA in regenerating wild-type and *sof*^{b123} fins. First we determined the relative expression of *cx43* and *cx40.8* in wild-type regenerating fins and found expression at similar levels (Fig. 3A). Next, we compared *cx40.8* levels in wild-type and *sof*^{b123} and found no substantial difference in expression levels of *cx40.8* (Fig. 3 and Table 1). At the same time, we followed *cx43* levels (previous studies revealed that *cx43* levels are reduced 15–20-fold in *sof*^{b123} compared to wild-type [12]). As before, we found that

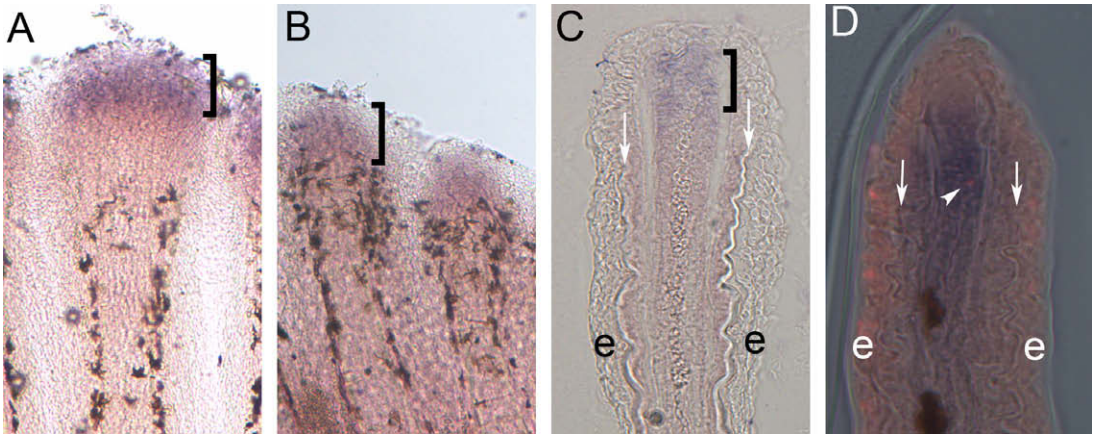

Fig. 2. Expression of *cx40.8* mRNA in zebrafish regenerating fins is consistent with *cx43* expression and the compartment of proliferating cells. (A) ISH of *cx40.8* in 5 dpa wild-type regenerating fins. (B) ISH of *cx40.8* in 5 dpa *sof*^{b123} regenerating fins. (C) Cryosection of stained wild-type regenerating fin showing *cx40.8* expression is located in the distal mesenchymal compartment. Brackets identify *cx40.8*-positive cells. (D) Cryosection of stained wild-type fin showing both *cx40.8* and co-localization with an H3P-positive cell. Arrows point to bone matrix. e, epidermis.

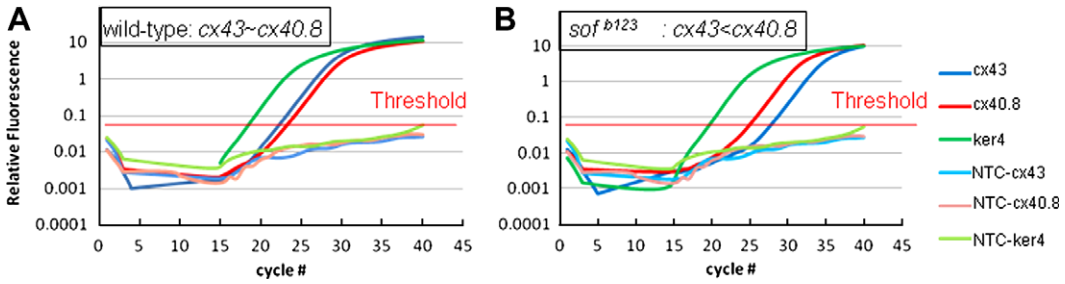

Fig. 3. Relative expression levels of *cx40.8* and *cx43* in regenerating fins. Data from representative wild-type (A) and *sof*^{b123} (B) fins are shown. (A) qRT-PCR of *cx43* and *cx40.8* levels relative to the internal standard, *ker4*. The amplicons for *cx43* and *cx40.8* are detected at similar cycle numbers (C_T), suggesting similar expression levels in wild-type. (B) In *sof*^{b123}, the *cx40.8* amplicon is detected at similar levels as in wild-type fins (see also Table 1), but *cx43* is detected much later (suggesting reduced mRNA levels in *sof*^{b123} fins). NTC, No transcript controls for each gene do not permit amplification.

Table 1
Expression levels of *cx40.8* are similar in wild-type and in *sof*^{b123} regenerating fins.

ΔΔCT values	Fold-change
cx40.8	
0.575	0.671
0.53	0.692
0.005	0.996

ΔΔCT values represent the relative expression of normalized *cx40.8* mRNA in *sof*^{b123} compared with wild-type. Fold-change values close to 1 suggests that the relative level of *cx40.8* is similar between wild-type and *sof*^{b123}.

cx43 levels are significantly reduced in *sof*^{b123} (Fig. 3). Since the level of *cx40.8* is unchanged in *sof*^{b123} while *cx43* is significantly reduced, the relative levels of *cx40.8* and *cx43* are drastically different between wild-type and *sof*^{b123}. Together, these data indicate that the transcription of *cx40.8* is not affected by reduced *cx43* mRNA. Moreover, the relative expression *cx40.8* is almost equal to *cx43* in wild-type fins, but it is 8–10-fold higher than *cx43* in *sof*^{b123} regenerating fins.

3.3. Cx40.8 fails to associate in gap junction plaques and does not form channels efficiently

Next, we sought to determine if Cx40.8 functions as a gap junction channel. HeLa cells transfected with an EGFP-tagged form of Cx40.8, Cx40.8-EGFP, revealed that Cx40.8 is localized primarily intracellularly and does not form detectable gap junction plaques at the plasma membrane (Fig. 4A and C). One possibility is that the EGFP-tagged zebrafish connexin protein is not trafficked normally using this heterologous system. While we cannot eliminate this possibility for Cx40.8-EGFP, previous studies have shown that zebrafish Cx43-EGFP is localized properly to the plasma membrane in gap junction plaques. Further, zebrafish Cx43-EGFP readily forms gap junction channels evidenced by transfer of the small dye propidium iodide in about 80% of the injected cell pairs [11]. To determine if Cx40.8 channels might be detected similarly, HeLa cells were transfected with Cx40.8-EGFP, and individual cells from transfected cell pairs were injected with propidium iodide. We found that 23.6% (±19.4) of cell pairs demonstrated dye transfer, suggesting that functional gap junction channels were formed, while most of the cell pairs fail to share dye (Fig. 4). Since it is possible to detect dye transfer, we suggest that Cx40.8 does not readily form gap junction channels, but channels that do form appear capable of GJIC.

3.4. Cx40.8 co-localizes with Cx43 in gap junction plaques

HeLa cell transfections showed that Cx40.8 is located intracellularly, albeit with the ability to form some gap junction channels at the plasma membrane. In an endogenous setting where Cx40.8 and Cx43 are co-expressed, Cx40.8 may have the opportunity to hetero-oligomerize or otherwise associate with Cx43. We investigated the possibility of an interaction between Cx40.8 and Cx43 by co-transfecting differentially tagged forms of Cx43 and Cx40.8.

We generated Cx43-mApple and Cx40.8-mApple constructs and found that they localized similarly to their EGFP counterparts.

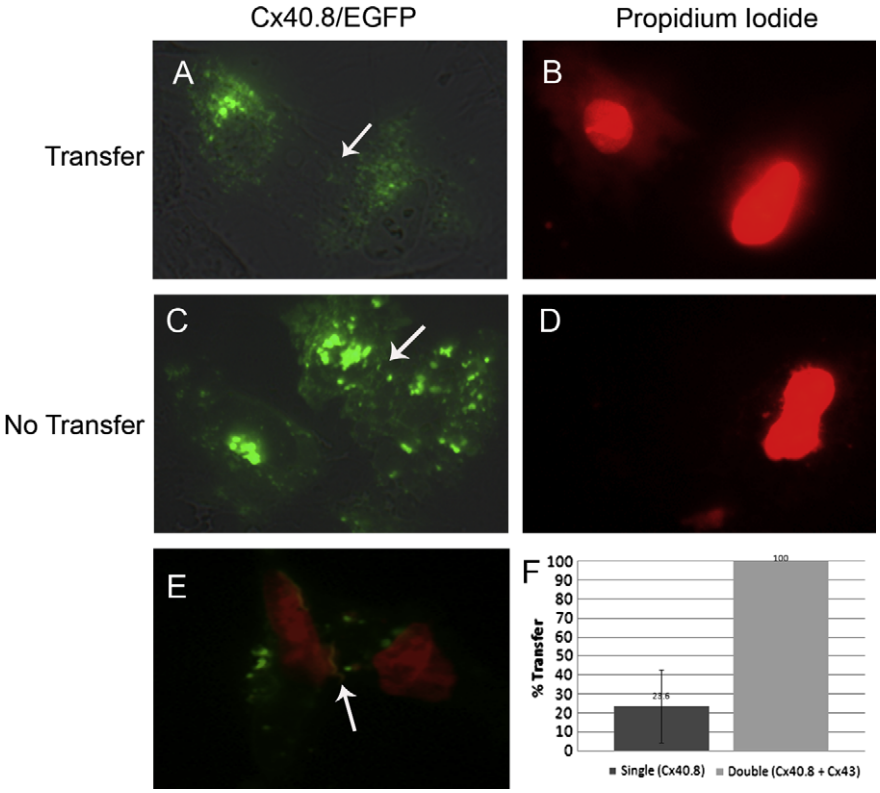

Fig. 4. Cx40.8 does not readily form gap junction channels when transfected alone. (A and B) An example of positive dye transfer in Cx40.8-EGFP transfected cell pairs. (C and D) An example of failure of dye transfer in Cx40.8-EGFP transfected cell pairs. Arrows point to plasma membranes of adjacent cells. (E) An example of positive dye transfer in HeLa cells co-transfected with Cx40.8-EGFP and Cx43-mAPPLE. Red and green images were overlaid, and the red image is slightly underexposed (compared to B and D) to insure visualization of the yellow gap junction plaque containing both connexins (arrow). (F) Quantitative analysis of positive dye transfer in singly-transfected Cx40.8-EGFP HeLa cells and doubly transfected HeLa cells. The data sets are significantly different ($P < 0.001$).

Next, we demonstrated that Cx40.8-EGFP and Cx40.8-mApple co-transfections resulted in yellow intracellular signal and Cx43-EGFP and Cx43-mApple co-transfections resulted in yellow plaques using confocal microscopy (not shown). Then, we co-transfected equal concentrations of Cx43-mApple with Cx40.8-EGFP, mimicking wild-type conditions (switching the fluorescent tags does not alter the results). Using confocal microscopy, cell pairs containing both green and red signals were first analyzed for the presence of Cx43 gap junction plaques. Cx43 plaques were then assessed for the presence of Cx40.8. Interestingly, among doubly-transfected cell pairs, all plaques containing Cx43 also contain Cx40.8 ($n = 15$ cell pairs, Fig. 5). This co-localization reveals that Cx40.8 (expressed mostly intracellularly when transfected alone) can be found in gap junction plaques when co-expressed with Cx43 and may suggest that Cx40.8 can hetero-oligomerize with Cx43. At this time, we cannot rule out the possibility that homomeric Cx40.8 channels more efficiently associate among homomeric Cx43-channels within the plaques. However, it is clear that the presence of Cx43 enhances the ability of Cx40.8 to localize in gap junction plaques at the plasma membrane.

Next we determined if the plaques containing both Cx43 and Cx40.8 permit dye transfer. Cells were co-transfected with Cx43-mApple and Cx40.8-EGFP prior to propidium iodide injection. Doubly-transfected cell pairs were identified by Cx40.8-EGFP positive plaques (i.e. since Cx40.8 is not found in plaques in singly-transfected cells). Interestingly, all of the injected cell pairs showed dye transfer (Fig. 4). At least two explanations are possible for the increased level of dye transfer in the double transfections over the Cx40.8-EGFP single transfections. First, it is apparent that Cx40.8 does not inhibit Cx43 channel function, so one possibility is that Cx40.8–Cx43 heteromeric channels are capable of transferring propidium iodide. Therefore, we do not rule out the hypothesis that Cx40.8 might directly modify the channel properties of Cx43 and enhance or alter the coupling of particular small molecules

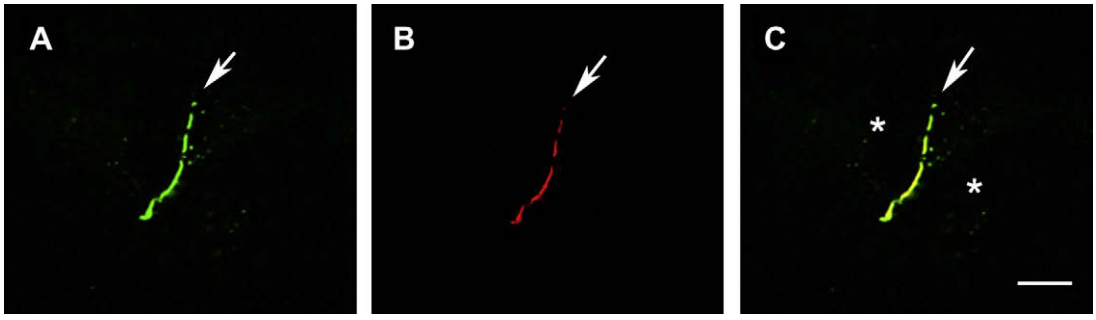

Fig. 5. Cx43 and Cx40.8 can associate together at the plasma membrane in HeLa cells. Cells were co-transfected with both Cx40.8-EGFP (A) and Cx43-mApple (B). Both connexins co-localize in gap junction plaques (C). Asterisks identify each cell in this cell pair.

(although further studies are required to demonstrate that channel properties differ among Cx40.8-channels, Cx43-channels, and heteromeric forms). Alternatively, the observed positive dye coupling may be permitted by homomeric forms of Cx43 and Cx40.8 gap junction channels. Indeed, Cx43 homomeric gap junction channels transfer propidium iodide efficiently [11], and such channels may exist within the plaques. Moreover, since co-transfection of Cx43 and Cx40.8 causes an increased association of Cx40.8 in gap junction plaques, and since we conclude above that Cx40.8 channels are capable of dye transfer, double transfection may simply increase the efficiency of bringing Cx40.8 to the plasma membrane where it can function as a typical channel. Future analyses using higher resolution imaging and ionic coupling assays are required to distinguish these possibilities.

4. Conclusions

Zebrafish Cx40.8 represents the closest connexin relative to Cx43. While the *cx40.8* gene is not found in mammalian genomes, the ODDD phenotypes may be caused by mutant forms of Cx43 modifying the function of wild-type Cx43 protein. Indeed, this study reveals that while *cx40.8* is expressed similarly to *cx43* in vivo, its function may be distinct. The Cx40.8 protein does not contribute to gap junction plaques efficiently on its own, but does in combination with Cx43. Therefore, when expression levels are similar (as in wild-type fins), Cx40.8 may have the opportunity to interact functionally with Cx43. However, when *cx40.8* is expressed at much higher levels than *cx43* (as in sof^{b123} fins), Cx40.8 may not be found at the plasma membrane. Therefore, it is possible that the reduced cell proliferation phenotype of *sof* mutants may be attributable to the absence of Cx40.8 at the plasma membrane, and/or due to the failure of Cx40.8-modification of Cx43 gap junction channels.

Acknowledgments

The authors thank Rebecca Jefferis for care of the zebrafish, Sarah Neilsen for the H3P and *cx40.8* co-localization studies, as well as Dr. Jutta Marzillier for her assistance with qRT-PCR. This research was funded by the NICHD (R01HD047737 to M.K.I.).

References

[1] Sohl, G. and Willecke, K. (2004) Gap junctions and the connexin protein family. Cardiovasc. Res. 62, 228–232.
[2] Laird, D.W. (2006) Life cycle of connexins in health and disease. Biochem. J. 394, 527–543.
[3] Bevans, C.G., Kordel, M., Rhee, S.K. and Harris, A.L. (1998) Isoform composition of connexin channels determines selectivity among second messengers and uncharged molecules. J. Biol. Chem. 273, 2808–2816.
[4] Elfgang, C., Eckert, R., Lichtenberg-Frate, H., Butterweck, A., Traub, O., Klein, R.A., Hulser, D.F. and Willecke, K. (1995) Specific permeability and selective formation of gap junction channels in connexin-transfected HeLa cells. J. Cell Biol. 129, 805–817.
[5] Goldberg, G.S., Valiunas, V. and Brink, P.R. (2004) Selective permeability of gap junction channels. Biochim. Biophys. Acta 1662, 96–101.
[6] Gerido, D.A. and White, T.W. (2004) Connexin disorders of the ear, skin, and lens. Biochim. Biophys. Acta 1662, 159–170.
[7] White, T.W. and Paul, D.L. (1999) Genetic diseases and gene knockouts reveal diverse connexin functions. Annu. Rev. Physiol. 61, 283–310.
[8] Paznekas, W.A. et al. (2003) Connexin 43 (GJA1) mutations cause the pleiotropic phenotype of oculodentodigital dysplasia. Am. J. Hum. Genet. 72, 408–418.
[9] Laird, D.W. (2008) Closing the gap on autosomal dominant connexin-26 and connexin-43 mutants linked to human disease. J. Biol. Chem. 283, 2997–3001.
[10] Iovine, M.K., Higgins, E.P., Hindes, A., Coblitz, B. and Johnson, S.L. (2005) Mutations in connexin43 (GJA1) perturb bone growth in zebrafish fins. Dev. Biol. 278, 208–219.
[11] Hoptak-Solga, A.D., Klein, K.A., Derosa, A.M., White, T.W. and Iovine, M.K. (2007) Zebrafish short fin mutations in connexin43 lead to aberrant gap junctional intercellular communication. FEBS Lett. 581, 3297–3302.
[12] Sims Jr., K., Eble, D.M. and Iovine, M.K. (2009) Connexin43 regulates joint location in zebrafish fins. Dev. Biol. 327, 410–418.
[13] Hoptak-Solga, A.D., Nielsen, S., Jain, I., Thummel, R., Hyde, D.R. and Iovine, M.K. (2008) Connexin43 (GJA1) is required in the population of dividing cells during fin regeneration. Dev. Biol. 317, 541–548.
[14] Iovine, M.K. and Johnson, S.L. (2000) Genetic analysis of isometric growth control mechanisms in the zebrafish caudal Fin. Genetics 155, 1321–1329.
[15] Poss, K.D., Keating, M.T. and Nechiporuk, A. (2003) Tales of regeneration in zebrafish. Dev. Dynam. 226, 202–210.
[16] Akimenko, M.A., Mari-Beffa, M., Becerra, J. and Geraudie, J. (2003) Old questions, new tools, and some answers to the mystery of fin regeneration. Dev. Dynam. 226, 190–201.
[17] Eastman, S.D., Chen, T.H., Falk, M.M., Mendelson, T.C. and Iovine, M.K. (2006) Phylogenetic analysis of three complete gap junction gene families reveals lineage-specific duplications and highly supported gene classes. Genomics 87, 265–274.
[18] Amores, A. et al. (1998) Zebrafish hox clusters and vertebrate genome evolution. Science 282, 1711–1714.
[19] Cao, F., Eckert, R., Elfgang, C., Nitsche, J.M., Snyder, S.A., DF, H.u., Willecke, K. and Nicholson, B.J. (1998) A quantitative analysis of connexin-specific permeability differences of gap junctions expressed in HeLa transfectants and Xenopus oocytes. J. Cell Sci. 111 (Pt. 1), 31–43.
[20] Bukauskas, F.F., Angele, A.B., Verselis, V.K. and Bennett, M.V. (2002) Coupling asymmetry of heterotypic connexin 45/connexin 43-EGFP gap junctions: properties of fast and slow gating mechanisms. Proc. Natl. Acad. Sci. USA 99, 7113–7118.
[21] Moreno, A.P. (2004) Biophysical properties of homomeric and heteromultimeric channels formed by cardiac connexins. Cardiovasc. Res. 62, 276–286.
[22] Westerfield, M. (1993) The Zebrafish Book: A Guide for the Laboratory Use of Zebrafish (*Brachydanio rerio*), University of Oregon Press, Eugene, OR.
[23] Wei, Y., Yu, L., Bowen, J., Gorovsky, M.A. and Allis, C.D. (1999) Phosphorylation of histone H3 is required for proper chromosome condensation and segregation. Cell 97, 99–109.